Vibration analysis and optimization of sandwich composite with curvilinear fibers

S Honda[1] and Y Narita[1]

[1] Division of Human Mechanical Systems & Design, Faculty of Engineering, Hokkaido University, Kita 13, Nishi 8, Sapporo, Hokkaido, 060-8628, Japan.

honda@eng.hokudai.ac.jp

Abstract. The present paper develops a shell element based on the refined zigzag theory (RZT) and applies it to the vibration analysis and optimization problem of the composite sandwich plate composed of CFRP skins and soft-cores. The RZT accepts large differences in layer stiffness, and requires less calculation effort than the layer-wise or three-dimensional theories. Numerical results revealed that the present method predicts vibration characteristics of composite sandwich plates with soft-core accurately. Then, shapes of reinforcing fibers in CFRP composite skins are optimized to maximize fundamental frequencies. As an optimizer, the particle swarm optimization (PSO) approach is employed since curvilinear fiber shapes are defined by continuous design variables. Obtained results showed that the composite sandwich with optimum curvilinear fiber shapes indicates higher fundamental frequencies compared with straight fibers.

1. Introduction

The passive constrained layer damping (PCLD) plate that forms a sandwich structure composed of stiff skins and soft-core layers is one of the effective vibration suppression elements since it requires no external actuators or heavy dampers and it shows excellent vibration suppression performance. This results in the wide range of applications of the PCLD plate in the automobile, marine, and aerospace structures [1]. In this study, the laminated fibrous composite plate with curvilinear reinforcing fibers is applied to skin layers and optimized their fiber shapes to maximize fundamental frequencies of sandwich plates. Laminates with curvilinear fibers are recently gathering attentions from many researchers and manufacturers since they indicate the higher performance in the specific situations compared with unidirectional straight or woven fibers [2], [3].

There is a difficulty to predict the vibration behavior of the sandwich plate with soft-core precisely by using the traditional laminated plate theories such as classical laminated plate theory (CLPT) [4] or

the first-order shear deformation theory (FSDT) [5] due to the large difference in the stiffness between skin layers and core material. The CLPT and FSDT assume the deformation of cross-section of laminated plate linearly and the PCLD plate indicates non-linear complex deformation shapes due to the core layer. To overcome this difficulty, many advanced laminated plate theories have been proposed. For example, the discrete layerwise theory (DLT) [6] and the three dimensional theory (3DT) [7] define displacements for each layer in the laminates and degree-of-freedoms (DOFs) in the thickness direction. These methods enable the precise prediction of the sandwich with soft-core but involve high calculation effort due to the rapid increase of DOFs. This is inappropriate to the optimization problem which requires a vast number of repeated calculation.

The refined zigzag theory (RZT) proposed by Tessler et. al. [8], [9] allows the expression of linearly varying displacement fields along each layer by modifying those of the FSDT with linear interpolation functions defined in each layer. This realizes the precise approximation for complex deformation of sandwich plate with soft-core compared with the CLPT and FSDT, and prevents increase of the calculation effort. There have been several studies on the application of the RZT. Iurlaro et. al. [10] compared the result from RZT with those from 3DT, FSDT, and HSDT in terms of free-vibration and buckling problem of composite sandwich plates. In our previous study [11], the authors proposed an analysis technique for composite sandwich plates with soft-cores based on the Ritz method with displacement functions that satisfy arbitrary combinations of boundary conditions, and maximized fundamental frequencies of the sandwich plate by optimizing lay-up configurations of composite skins. Finite elements based on the RZT are also proposed from many researchers [12]-[14]. However, elements proposed in those studies are one-dimensional beam or triangle shell elements, and so far no study proposes quadratic rectangular elements based on the RZT.

The present study proposes an iso-parametric 8-node quadratic rectangular element and applies it to optimization problems of curvilinear fiber shapes in skin layers. The curvilinear fibers are expressed by the cubic polynomial functions and coefficients of each term are assigned as design variables. The particle swarm optimization (PSO) method is used as an optimizer since it accepts continuous design variables. The numerical results calculated by the present shell element indicate good agreement with those from solid elements, and obtained optimum fiber shapes result in higher fundamental frequencies than those with straight fibers.

2. Numerical analysis and optimization method

2.1. Refined zigzag theory

A symmetrically laminated *N*-layer plate with dimensions $a \times b \times h$ (h: thickness) is considered. Displacements in the x, y, and z directions are denoted by u, v, and w. The superscript (k) indicates the physical quantities in the k-th layer of the plate.

Based on the RZT [8]-[9], displacements in the k-th layer are defined by

$$\begin{aligned} u^{(k)}(x,y,z) &= u(x,y) + z\alpha_x(x,y) + \phi_x^{(k)}(z)\psi_x(x,y) \\ v^{(k)}(x,y,z) &= v(x,y) + z\alpha_y(x,y) + \phi_y^{(k)}(z)\psi_y(x,y) \\ w^{(k)}(x,y,z) &= w(x,y) \end{aligned} \tag{1}$$

where $u(x, y)$, $v(x, y)$ and $w(x, y)$ are the displacements in the mid-plane of the plate, $\alpha_x(x, y)$ and $\alpha_y(x, y)$ are the angles between the surface normal to the mid-plane and the deformed surface due to the shear deformation in each direction. These variables are common with the FSDT, and these are corrected by $\phi_x^{(k)}(z)\Psi_x(x, y)$ and $\phi_y^{(k)}(z)\Psi_y(x, y)$ in the RZT. The functions $\phi_x^{(k)}(z)$ and $\phi_y^{(k)}(z)$ are the zigzag functions which are piecewise linear in each layer, and the functions $\Psi_x(x, y)$ and $\Psi_y(x, y)$ are amplitudes of the zigzag functions which determine the magnitude of the effectiveness of the correction terms.

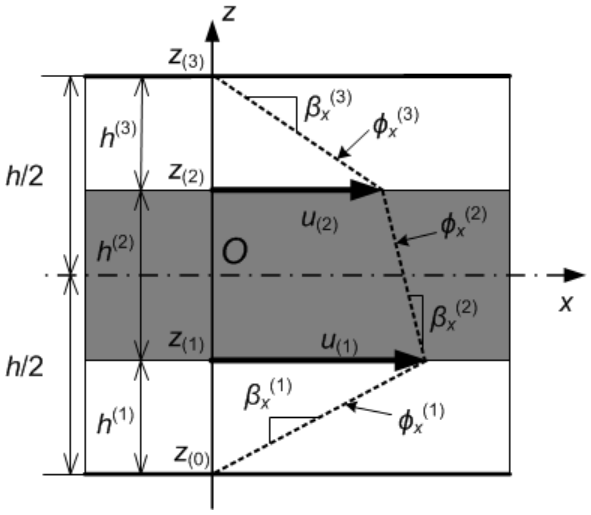

Figure 1. Notation of zigzag function for the 3-layer laminate.

An example of the zigzag function ϕ_x of the symmetric 3-layer laminate in the x direction is shown in figure 1, where $z^{(k)}$ is the z coordinate of the upper surface of the k-th layer, $u^{(k)}$ and $v^{(k)}$ are the magnitudes of the zigzag functions $\phi_x^{(k)}(z)$ and $\phi_y^{(k)}(z)$ at $z = z^{(k)}$, and $\beta_x^{(k)}$ and $\beta_y^{(k)}$ are the gradients of the zigzag function in the k-th layer.

The zigzag functions in the x and y directions $\phi_x^{(k)}(z)$ and $\phi_y^{(k)}(z)$ are given by

$$\phi_x^{(1)}(z) = \left(z + \frac{h}{2}\right)\beta_x^{(1)} = \left(z + \frac{h}{2}\right)\left(\frac{G_x}{\bar{Q}_{55}^{(1)}} - 1\right) \quad (k = 1)$$
$$\phi_x^{(k)}(z) = \left(z - z_{(k-1)}\right)\beta_x^{(k)} + u_{(k-1)} = \left(z + \frac{h}{2}\right)\left(\frac{G_x}{\bar{Q}_{55}^{(k)}} - 1\right) + \sum_{i=2}^{k} h^{(i-1)}\left(\frac{G_x}{\bar{Q}_{55}^{(i-1)}} - \frac{G_x}{\bar{Q}_{55}^{(k)}}\right) \quad (k \geq 2) \tag{2}$$

$$\phi_y^{(1)}(z) = \left(z + \frac{h}{2}\right)\beta_y^{(1)} = \left(z + \frac{h}{2}\right)\left(\frac{G_y}{\bar{Q}_{44}^{(1)}} - 1\right) \quad (k = 1)$$
$$\phi_y^{(k)}(z) = \left(z - z_{(k-1)}\right)\beta_y^{(k)} + u_{(k-1)} = \left(z + \frac{h}{2}\right)\left(\frac{G_y}{\bar{Q}_{44}^{(k)}} - 1\right) + \sum_{i=2}^{k} h^{(i-1)}\left(\frac{G_y}{\bar{Q}_{44}^{(i-1)}} - \frac{G_y}{\bar{Q}_{44}^{(k)}}\right) \quad (k \geq 2) \tag{3}$$

where $\bar{Q}_{44}^{(k)}$ and $\bar{Q}_{55}^{(k)}$ are the transformed elastic moduli in the transverse directions with respect to the material principle axes, and G_x and G_y are also defined by using those, as follows.

$$G_x = \left(\frac{1}{h}\sum_{k=1}^{N}\frac{h^{(k)}}{\bar{Q}_{55}^{(k)}}\right)^{-1}, \quad G_y = \left(\frac{1}{h}\sum_{k=1}^{N}\frac{h^{(k)}}{\bar{Q}_{44}^{(k)}}\right)^{-1} \tag{4}$$

It is known from equation (4) that the zigzag functions $\phi_x^{(k)}(z)$ and $\phi_y^{(k)}(z)$ are defined by material constant and thickness of each layer. The present study limits the plate to symmetric laminate, and thus the coupling of the stretching and bending deformation is cancelled, resulting in five independent variables, w, α_x, α_y, Ψ_x, and Ψ_y.

2.2. Finite element based on the RZT

The present study limits the plate to symmetrical laminate, and coupling between in-plane and out-of-plane direction is cancelled. The bending stiffness **D** and shear stiffness **G** are only used to calculate natural frequencies. The resultant stress and strain relation of symmetrically laminated plate in the out-of-plane direction is given as follows.

$$\begin{Bmatrix}\mathbf{M}_b\\ \mathbf{Q}_s\end{Bmatrix}=\begin{bmatrix}\mathbf{D} & 0\\ 0 & \mathbf{G}\end{bmatrix}\begin{Bmatrix}\mathbf{e}_b\\ \mathbf{e}_s\end{Bmatrix}=\mathbf{D}_t\boldsymbol{\kappa} \tag{6}$$

where $\mathbf{M}_b$ and $\mathbf{Q}_s$ are resultant moment and shear force vectors, and $\mathbf{e}_b$ and $\mathbf{e}_s$ are the curvature and shear strain vectors. **G** is defined with the gradient of zigzag function β_x and β_y as follows.

$$\mathbf{G}=\int_{-h/2}^{h/2}\begin{bmatrix}\overline{Q}_{44} & \beta_y\overline{Q}_{44} & \overline{Q}_{45} & \beta_x\overline{Q}_{45}\\ & \beta_y^2\overline{Q}_{44} & \beta_y\overline{Q}_{45} & \beta_x\beta_y\overline{Q}_{45}\\ & & \overline{Q}_{55} & \beta_x\overline{Q}_{55}\\ sym. & & & \beta_x^2\overline{Q}_{55}\end{bmatrix}^{(k)}dz \tag{7}$$

The element strain energy U_e and kinematical T_e energy are given as

$$U_e=\frac{1}{2}\int_{A_e}\boldsymbol{\kappa}^{\mathrm{T}}\mathbf{D}_t\boldsymbol{\kappa}dA_e=\frac{1}{2}\boldsymbol{\delta}_e^{\mathrm{T}}\mathbf{K}_e\boldsymbol{\delta}_e \tag{8}$$

$$T_e=\frac{1}{2}\sum_{k=1}^{N}\rho^{(k)}\int_{V_{e_k}}\left[\left(\frac{\partial u}{\partial t}\right)^2+\left(\frac{\partial v}{\partial t}\right)^2+\left(\frac{\partial w}{\partial t}\right)^2\right]^{(k)}dV_{e_k}=\frac{1}{2}\omega^2\boldsymbol{\delta}_e^{\mathrm{T}}\mathbf{M}_e\boldsymbol{\delta}_e \tag{9}$$

where A_e is element area, $\boldsymbol{\delta}_e$ is element displacement vector, and $\mathbf{K}_e$ and $\mathbf{M}_e$ are the element stiffness and mass matrixes.

After assembling energies of all elements and minimizing the total potential energy, the frequency equation is obtained as follows.

$$\left|\mathbf{K}-\omega^2\mathbf{M}\right|=0 \tag{10}$$

where **K** and **M** are total stiffness and mass matrixes and ω is angular frequency. Using the material constants of skins and the reference stiffness $D_0 = E_2h^3 / 12(1-\nu_{12}\nu_{21})$, the obtained frequency is normalized as follows.

$$\Omega=\omega a^2\left(\frac{\rho h}{D_0}\right)^{1/2} \tag{11}$$

where Ω is the non-dimensional frequency or frequency parameter.

2.3. Expression of curvilinear fiber shape

A cubic polynomial function $f(x,y)$ is introduced to define curvilinearly shaped fibers, as

$$f(x,y) = c_{00} + c_{10}x + c_{01}y + c_{20}x^2 + c_{11}xy + c_{02}y^2 + c_{30}x^3 + c_{21}x^2y + c_{12}xy^2 + c_{03}y^3 \tag{12}$$

where c_{ij} (i, j = 0, 1, 2, 3) are shape coefficients which determine the surface shape. An example of a surface and the corresponding curves are shown in figure 2(a), and figure 2(b) indicates contour lines of the surface projected on the horizontal plane. A range of shapes of surfaces could be described with this expression by varying the values of the coefficients c_{ij}. It is difficult to employ continuously curved fibers in the FEA, and the fibers are discretised at each element and dealt with as straight fibers. The fiber orientation angle $\theta_{n,p}$ at the p-th element in the n-th layer is defined as the tangential direction of the contour lines using the coordinates $(x_c, y_c)_p$ of the center of the element, which is calculated using the following equation.

$$\theta_{n,p}(x_c, y_c) = \tan^{-1}\left(-\frac{\partial f / \partial x}{\partial f / \partial y}\right)\Bigg|_{x=x_c, y=y_c} \tag{13}$$

It is assumed that each element has a straight fiber with a constant volume fraction but different orientation angle, and the discrete shape of figure 2(b) is shown in figure 2(c). The angles are defined by a continuous polynomial function and this description imposes continuity constraints on the fiber directions between neighbouring elements. The present description accepts closed shapes which may be effective to reinforce the around circles.

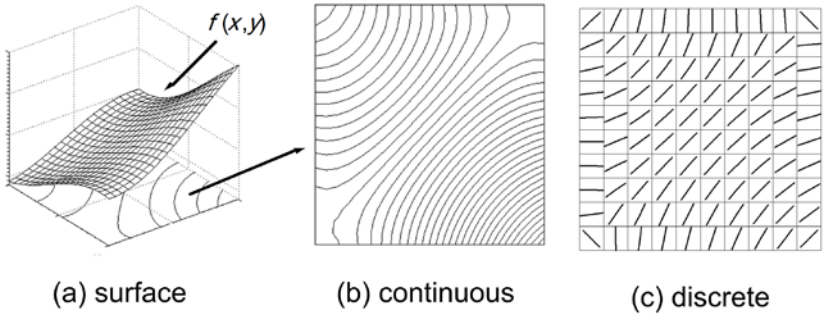

Figure 2. Example of curvilinear fiber expression.

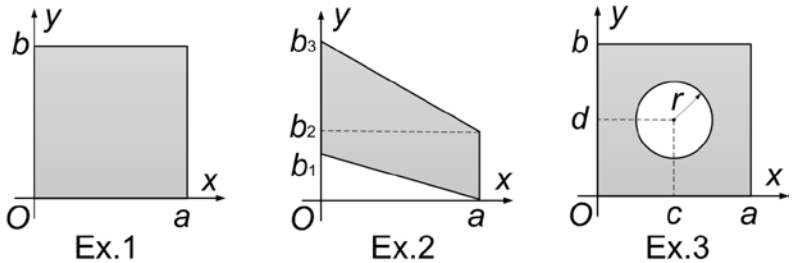

Figure 3. Plate shapes and dimensions

Table 1. The lowest three natural frequencies obtained from the SOLID, the FSDT, and the present RZT for three models.

Model	Dimension [mm]	Mode	Natural frequency [Hz]		
			SOLID	FSDT	RZT
Ex.1	$a = b = 150$, $h = 15$	1st	2021	4487	2032
		2nd	2657	5805	2667
		3rd	3732	8119	3742
Ex.2	$a = b_3 = 150$, $b_1 = 30$, $b_2 = 60$, $h = 15$	1st	446	849	446
		2nd	1001	2022	1003
		3rd	1915	4182	1925
Ex.3	$a = b = 150$, $c = d = 75$, $r = 37.5$, $h = 15$ mm.	1st	2843	6282	2855
		2nd	2879	6347	2890
		3rd	4244	8403	4299

Table 2. Material constants for graphite/epoxy (CFRP) and polyvinyl chloride (P).

Material	Values
CFRP	$E_1 = 138$ GPa, $E_2 = 8.96$ GPa, $\nu_{12} = 0.30$, $\rho = 1578$ kg/m^3
Polyvinyl chloride (P)	$E = 0.104$ GPa, $\nu = 0.30$, $\rho = 1400$ kg/m^3

3. Numerical results

3.1. Accuracy of the present calculation method

Figure 3 shows shapes of the composite sandwich plates employed as examples in this study. Example 1 is the square plate, example 2 is wing shaped plate, and example 3 is the plate with a hole at the center. Dimensions of each example are listed in table 1. Materials are assumed as graphite/epoxy or CFRP composites for skins and polyvinyl chloride (P) for soft-cores, and those material constants are listed in table 2 where E_1 and E_2 are the Young's moduli in the fiber and normal to the fiber directions. ν_{12} is the Poisson's ratio in the corresponding direction, and ρ is material density.

To validate the present RZT element, the results are compared with those from the SOLID element and shell element formulated by the FSDT. Boundary conditions for each pate are that examples 1 and 3 are totally clamped plate and example 2 is the cantilever with the clamped left edge. From preliminary mesh study, the numbers of meshes for examples 1 and 3 are decided to 10 × 10, and example 2 to 9 × 15 in the in-plane direction. The number of meshes for the SOLID model in the thickness direction is six, and meshes for the in-plane direction are same with shell models. The final size of matrixes used in eigenvalue calculation for example 1 becomes 9339 × 9339 for SOLID, 1023 × 1023 for FSDT, and 1705 × 1705 for RZT. That is, the present RZT requires only 3.33 % sized matrix for eigenvalue calculation compared with SOLID model, resulting in low calculation effort.

Table 1 lists the lowest three natural frequencies for three examples. Unidirectional, 0°, CFRP skins are used for both sides [0/P/0] and thickness of each layer is equal, 5 + 5 + 5 = 15 mm.

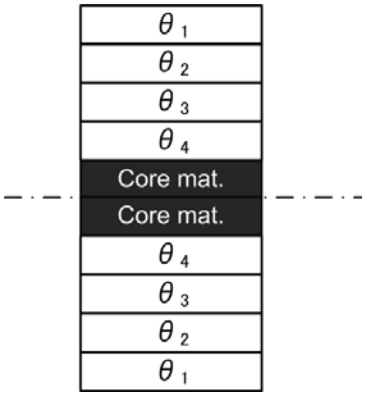

Figure 4. Cross-sectional lay-out of the optimization problem.

From table 1, all frequencies results in good agreement between SOLID and RZT, but the FSDT gives much higher frequencies than others. This is because the FSDT approximates deformation in the thickness direction linearly for whole thickness, and could not express the complex deformation of soft-core in the composite sandwich, which assumes the equivalent stiffness for whole thickness higher than those really have. The present method has 3.33 % matrix size compared with solid element and indicates good agreement with the solid element in terms of deriving natural frequencies. Therefore, the validity and effectiveness of the present method are confirmed from these comparison.

3.2. Optimization problem

3.2.1. Optimization conditions. It is known from the past study [2] that the curvilinear fibers have advantages for unsymmetrical boundary conditions over symmetrical ones. So, the optimization results are given for common examples with section 3.2 but the different boundary condition for examples 1 and 3, which is the clamped, simply supported, free, and free edges with the point-supported upper-right corner where the direction is from plate left edge in the counter-clockwise direction. A lay-up condition of the sandwich plate is described in figure 4. It has symmetric eight skin layers with equal thicknesses and twice thickness in the core material.

The present optimization problem can be formulated as follows.

Maximizing: Ω_1 fundamental frequency parameter

Design variables: $c_{ij}^{(k)}$ (i, j = 0, 1, 2, 3; k = 1, 2, 3, 4)

Subject to: $c_{00} = 0.0$

where $c_{ij}^{(k)}$ are the coefficients of each term in equation (12) of the k-th layer. The design variables are continuous numbers here, and the particle swarm optimization (PSO) method is employed as an optimizer. The PSO is one of the effective meta-heuristic solutions and mimics behaviour of flock of birds or fish. Many particles expressing solutions move around in the solution space with interactions each other and search the promising region precisely. The position vector $\mathbf{x}_m(t)$ of particle m at the t-th research is updated by

$$\mathbf{x}_m(t+1) = \mathbf{x}_m(t) + \mathbf{v}_m(t+1) \tag{14}$$

where $\mathbf{v}_m(t)$ is the velocity vector and is updated by

$$\mathbf{v}_m(t+1) = W\mathbf{v}_m(t) + C_1 r_1(\mathbf{x}_{pbest,\,m} - \mathbf{x}_m(t)) + C_2 r_2(\mathbf{x}_{gbest} - \mathbf{x}_m(t)) \tag{15}$$

where $\mathbf{x}_{pbest,\,m}$ is the personal best of m-th particle and $\mathbf{x}_{gbest}$ is the global best solution found during the past all iterations. Due to this, interactions between solutions are kept. The coefficient r_1 and r_2 are the random numbers from 0 to 1, and W, C_1 and C_2 are weight coefficients to be defined by the operator. In the present optimization problem, the following PSO parameters are used, and these values are determined based on the numerical experiments.

The number of particles	N_p = 100
The number of iterations	T = 100
Weight coefficients	W = 0.5, C_1= C_2= 0.9

Table 3. Maximum fundamental frequencies for three examples from curvilinear and linear fibers.

No.	Frequency parameter [-]		Optimum lay-up with straight fiber	Improvement [%]
	Curvilinear opt.	Straight opt.		
Ex. 1	16.44	14.76	[45/-75/-75/45]s	11.37
Ex. 2	8.063	7.941	[-15/-15/-15/-15]s	1.54
Ex. 3	16.66	15.27	[75/15/90/30]s	9.07

3.2.2. Optimization results. Table 3 lists maximized fundamental frequency parameters Ω_1 of three examples for the plates with the present curvilinear and with the traditional straight fibers, optimum lay-ups for plates with straight fibers that are obtained by using the layerwise optimization (LO) method [11], and improvement ratios based on straight fibers. The frequency parameter Ω_1 is normalized frequency defined by equation (11). Obtained optimum curvilinear fiber shapes that are discretised in each element are indicated in figure 5, and corresponding coefficients of equation (11) for each layer are detailed in table 4.

It is known from table 3 that the present plates show higher fundamental frequencies than the straight fibers for all examples, and thus curvilinear fibers reinforce the composites including sandwich plate with soft-core effectively compared with traditional straight fibers. Improvements are about ten percent for examples 1 and 3, and a small improvement is obtained in example 2. This is because example 2 has the simple boundary condition and consequently it results in the simple vibration mode shape. The first vibration mode shapes for three examples are given in figure 6. Examples 1 and 3 have asymmetric boundary condition and show complex contours. The fibers in the first and third layers orient normally to the clamped left edge and incline to other edges. To suppress the deformation of plate, fibers are across peaks of contour (red parts) normally in the most layers. The stream of fibers from clamped and simply supported edges to the point-supported corner is also seen in the first layer. In contrast with these, in example 2, obtained fiber shapes show low curvatures and are close to the straight fibers. From these, it is revealed as with [2] that the curvilinear fibers are effective especially for the plate with complex deformation shape since curved fibers form flexibly to the deformation shape and suppress it effectively.

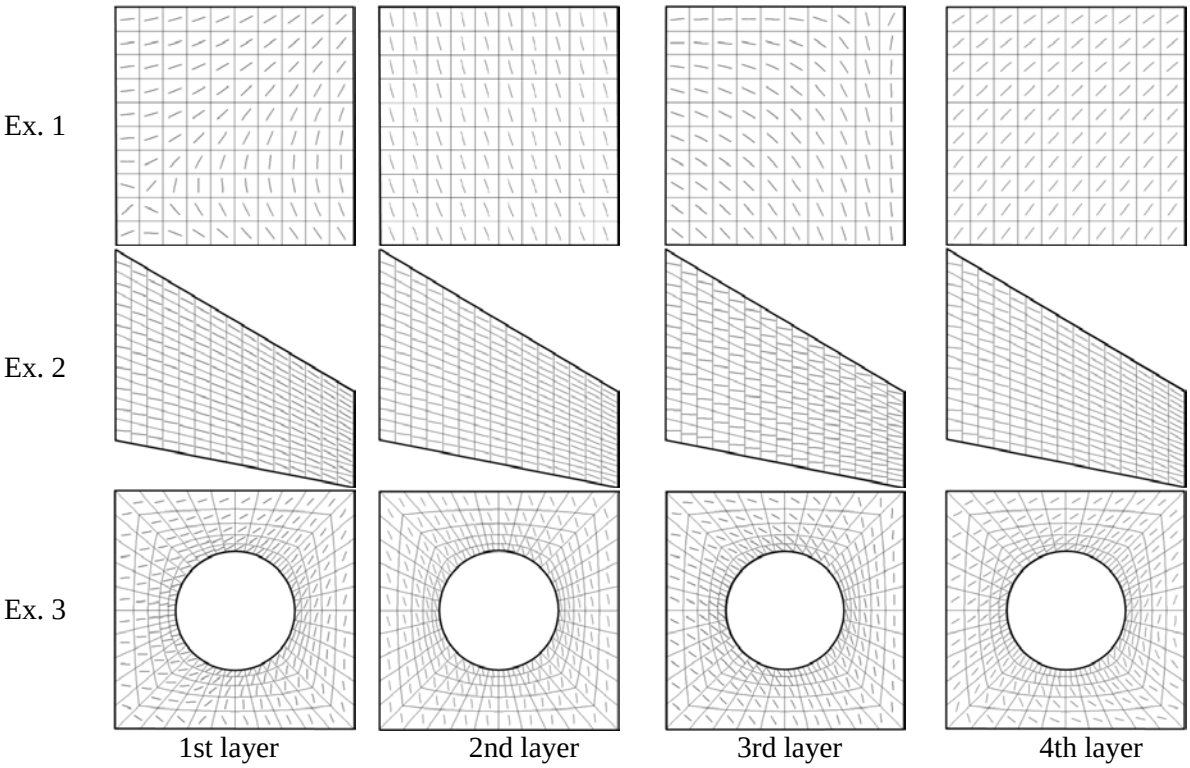

Figure 5. Optimum fiber shapes discretiezed in each element for symmetric 8-layer skins.

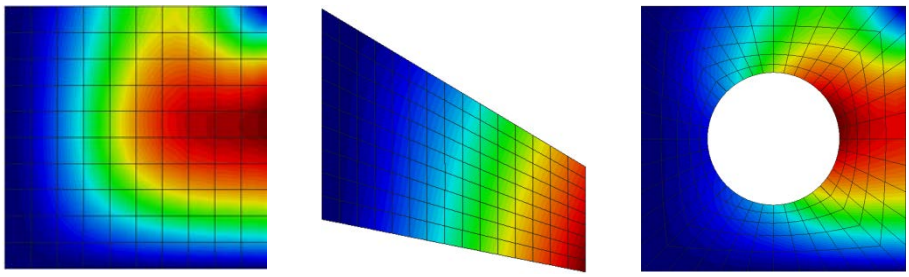

Figure 6. Vibration mode shapes for the three sandwich plates with optimum curvilinear fiber shapes.

4. Conclusions

The present study proposed a new shell element based on the refined zigzag theory that accepted large differences between laminates and saved the increase of degree-of-freedom (DOF). Then, the element was applied to the optimization problem of composite sandwich with curvilinear reinforcing fibers in the skin layers. Curvilinear fibers were expressed by using the cubic polynomial surface, and each coefficient of polynomials were used as design variables. The objective function to be maximized was fundamental frequencies of sandwich plates. The particle swarm optimization (PSO) was employed as an optimizer since it accepted continuous design variables and had high convergence property.

From numerical experiments, the present element indicated the similar calculation accuracy with the solid element in terms of natural frequencies of composite sandwich with soft-core, and the calculation effort of the present method was quite small compared with the solid element. Optimized fiber shapes resulted in higher fundamental frequencies than the straight fibers since they formed their shape flexibly and effectively to suppress the deformation of the structures. Therefore, it was

concluded that the proposed element is useful to predict and design the vibration characteristics of the composite sandwich plates with soft-cores.

Table 4. Coefficient of each term for optimum fiber shapes.

No.	Layer	Opt. shape coefficient c_{ij}								
		c_{10}	c_{01}	c_{20}	c_{11}	c_{02}	c_{30}	c_{21}	c_{12}	c_{03}
Ex.1	1st	0.10	-0.17	-2.13	-1.39	3.04	-0.06	0.23	0.36	3.49
	2nd	4.55	1.77	-0.01	0.95	-3.16	1.42	-6.65	0.68	1.80
	3rd	2.96	3.64	2.43	-22.54	-0.95	0.79	1.23	-1.56	-6.15
	4th	-5.08	3.83	0.64	-2.75	4.68	1.01	-1.77	1.76	31.87
Ex.2	1st	0.02	1.66	3.03	1.92	-3.23	1.07	1.86	0.49	1.41
	2nd	0.11	2.48	2.33	4.57	-2.29	8.20	5.78	-2.13	0.56
	3rd	-0.24	2.85	1.65	7.41	3.04	2.82	2.91	0.29	3.48
	4th	-0.07	1.35	3.70	2.81	1.03	-1.70	7.53	-7.93	-9.65
Ex.3	1st	0.33	0.37	1.02	-8.17	9.26	-45.19	-9.76	13.38	1.79
	2nd	2.25	0.24	7.14	0.08	2.04	-0.08	2.68	-1.71	9.48
	3rd	1.50	1.78	2.25	-10.32	-1.11	1.46	-3.12	1.70	-1.13
	4th	-1.68	-0.82	0.68	-54.83	68.24	1.88	-0.07	1.41	1.08

References

[1] Castel A, Loredo A, Hafidi A E, Martin B, Complex power distribution analysis in plates covered with passive constrained layer damping patches, Journal of Sound and Vibration, Vol. 331 (2012) 2485-2498.
[2] Honda S, Igarashi T, Narita Y, Multi-objective optimization of curvilinear fiber shapes for laminated composite plates by using NSGA-II", Composites Part B: Engineering, Vol. 45, (2013) 1071-1078.
[3] Lopes C S, Gürdal Z, Camanho P P, Variable-stiffness composite panels: Buckling and first-ply failure improvements over straight-fiber laminates. Computational Structure Vol. 86, No. 9, (2008) 897-907.
[4] Leissa A W, Vibration of Plates, NASA-160, U.S. Government Printing Office, Washington, DC, 1969.
[5] Reddy J N, Mechanics of laminated composite plates, CRC Press, Inc. New York, 1997
[6] Hung K H, Dasgupta A, A layer-wise analysis for free vibration of thick composite cylindrical shells, Journal of Sound and Vibration, Vol. 186 (1995) 207-222.
[7] Kang J H, Leissa A W, Three-dimensional vibration analysis of thick hyperboloidal shells of revolution, Journal of Sound and Vibration, Vol. 282 (2005) 277-296.
[8] Tessler A, Sciuva M D, Gherlone M, Refined zigzag theory for laminated composite, and sandwich plates, NASA Technical Reports, NASA/TP (2009), 215561.
[9] Tessler A, Sciuva M D, Gherlone M, Refined zigzag theory for homogeneous, laminated composite, and sandwich plates: a homogeneous limit methodology for zigzag function selection, NASA Technical Reports, NASA/TP (2010), 216214.
[10] Iurlaro L, Gherlone M, M. Sciuva D, Tessler A, Assessment of the refined zigzag theory for bending, vibration, and buckling of sandwich plates: a comparative study of different theories, Composite Structures, Vol. 106 (2013) 777-792.
[11] Honda S, Kumagai T, Tomihashi K, Narita Y, Frequency maximization of laminated sandwich plates under general boundary conditions using layerwise optimization method with refined

zigzag theory, Journal of Sound and Vibration, Vol. 332 (2013) 6451-6462.
[12] Gherlone M, Tessler A, Sciuva M D, C0 beam elements based on the refined zigzag theory for multilayered composite and sandwich laminates, Composite Structures, Vol. 93 (2011) 2882-2894.
[13] Versino D, Gherlone M, Mattone M, Sciuva M D, Tessler A, C0 triangular elements based on the Refined Zigzag Theory for multilayer composite and sandwich plates, Composite: Part B, Vol. 44 (2013) 218-230.
[14] Barut A, Madenci E, Tessler A, C0-continuous triangular plate element for laminated composite and sandwich plates using the {2,2} – Refined Zigzag Theory, Composite Structures, Vol. 106 (2013) 835-853.